

Constrained Parameter Inference as a Principle for Learning

Nasir Ahmad Ellen Schrader Marcel van Gerven
 Department of Artificial Intelligence
 Donders Institute for Brain, Cognition and Behaviour
 Radboud University, Nijmegen, the Netherlands

Abstract

Learning in biological and artificial neural networks is often framed as a problem in which targeted error signals guide parameter updating for more optimal network behaviour. Backpropagation of error (BP) is an example of such an approach and has proven to be a highly successful application of stochastic gradient descent to deep neural networks. However, BP relies on the global transmission of gradient information and has therefore been criticised for its biological implausibility. We propose constrained parameter inference (COPI) as a new principle for learning. COPI allows for the estimation of network parameters under the constraints of decorrelated neural inputs and top-down perturbations of neural states. We show that COPI is not only more biologically plausible but also provides distinct advantages for fast learning, compared with the backpropagation algorithm.

1 Introduction

Learning can be defined as the ability of natural and artificial systems to adapt to changing circumstances based on their experience. In biological and artificial neural networks this requires updating of the parameters that govern the network dynamics [29].

A principled way of implementing learning in artificial neural networks is through the backpropagation of error (BP) algorithm [1, 7]. BP is a gradient-based method which uses reverse-mode automatic differentiation to compute the gradients that are needed for parameter updating [24]. This approach relies on the repeated application of forward and backward passes through the network. In the forward (inference) pass, network activity is propagated forward to compute network outputs. In the backward (learning) pass, the loss gradient associated with the network outputs is propagated in the reverse direction for parameter updating.

While effective, BP makes use of the global transmission of gradients using biologically implausible non-local operations. [3, 4, 32]. Alternative approaches, such as Hebbian learning and subspace methods circumvent this problem yet are restricted to unsupervised learning and do not afford (deep) credit assignment [16, 19].

Here, instead, we propose constrained parameter inference (COPI) as a new principle for learning. COPI uses information that is locally available at the synapse under the constraints of decorrelated inputs and top-down perturbations that guide learning. Note that COPI is distinct from methods that rely on measuring gradients through activity differences (see the NGRAD hypothesis [32]), in that no difference in activity needs to be computed to determine parameter updates. Instead, all updates are inferences of the desired transformation.

One may ask what form this perturbation should take in order to produce effective credit (or rather activity) assignment and thereby effective learning. In this work, we propose that the form of the perturbation determines which learning algorithm is being used for learning within the system. Particularly, this approach can leverage credit assignment of any form, whether based on backpropagation, feedback alignment [21, 22], target propagation [13, 31] or otherwise.

In the following, we demonstrate that COPI provides a powerful framework for learning which is at least as effective as backpropagation of error while having the potential to rely on local

operations only. This has direct implications for modern machine learning as COPI can be used as a plug-in replacement of backpropagation in a wide range of settings.

2 Methods

In this section, we develop the constrained parameter inference (COPI) approach and describe its use for parameter estimation in feedforward neural networks.

2.1 Deep neural networks

Let us consider deep neural networks consisting of L layers. The input-output transformation in layer l is given by

$$y_l = f(a_l) = f(W_l x_l)$$

with output y_l , activation function f , activation $a_l = W_l x_l$, input x_l and weight matrix $W_l \in \mathbb{R}^{K_l \times K_{l-1}}$, where K_l indicates the number of units in layer l . As usual, the input to a layer $l > 1$ is given by the output of the previous layer, that is, $x_l = y_{l-1}$. Learning in deep neural networks amounts to determining for each layer in the network a weight update Δ_{W_l} such that the update rule

$$W_l \leftarrow W_l + \eta \Delta_{W_l}$$

converges towards those weights that minimize a loss ℓ for some dataset \mathcal{D} for some suitable learning rate $\eta > 0$. Locally, the optimum by gradient descent (GD) is to take a step in the direction of the negative expected gradient of the loss. That is,

$$\Delta_{W_l}^{\text{gd}} = -\mathbb{E}[\nabla_{W_l} \ell],$$

where, in practice, the expectation is taken under the empirical distribution.

2.2 Constrained parameter inference in feedforward systems

Here, we develop an alternative approach and relate it directly to both stochastic gradient descent and local parameter inference. The key transformation in a deep feedforward neural network is carried out by a weight matrix given by

$$a_l = W_l x_l.$$

Suppose we know the desired target state z_l for this transformation. This can be expressed as an alternative transformation

$$z_l = D_l x_l$$

for some desired weight matrix D_l . Ideally, we would use a learning algorithm which could guarantee a convergence of the current weight matrix. A straightforward proposal is to carry out a decay from the current weight values to the desired weight values, such that the weight update is of the form

$$\Delta_{W_l} = \mathbb{E}[D_l - W_l] = D_l - W_l. \tag{1}$$

The key goal is to achieve this weight update without making use of the (unknown) desired weight matrix.

2.3 Learning the forward weights

Let us rewrite the desired weight matrix in the following way:

$$\begin{aligned} D_l &= D_l \left(\mathbb{E}[x_l x_l^\top] \mathbb{E}[x_l x_l^\top]^{-1} \right) \\ &= \mathbb{E}[D_l x_l x_l^\top] \mathbb{E}[x_l x_l^\top]^{-1} \\ &= \mathbb{E}[z_l x_l^\top] \mathbb{E}[x_l x_l^\top]^{-1} \end{aligned}$$

with $\mathbb{E}[x_l x_l^\top]$ the expected (empirical) correlation matrix, which we assume to be invertible, though this condition is relaxed later. If we plug this back into Eq. (1) then we obtain

$$\Delta_{W_l} = \mathbb{E}[z_l x_l^\top] \mathbb{E}[x_l x_l^\top]^{-1} - W_l, \quad (2)$$

allowing the weight update to be expressed in terms of target outputs rather than (unknown) desired weights.

Let us assume for the moment that the inputs x_l are distributed such that they have zero covariance and unit variance, i.e., the inputs are whitened. This implies that the expected correlation matrix is given by the identity matrix, that is, $\mathbb{E}[x_l x_l^\top] = I$. In this case, Eq. (2) reduces to the simple update rule

$$\Delta_{W_l} = \mathbb{E}[z_l x_l^\top] - W_l.$$

In practice, it may be unreasonable (and perhaps even undesirable) to assume perfectly whitened input data. A more realistic and achievable scenario is one in which we make the less restrictive assumption that the data is decorrelated rather than whitened. This implies that the expected correlation matrix is diagonal, that is, $\mathbb{E}[x_l x_l^\top] = \text{diag}(\mathbb{E}[x_l^2])$. Here, $x_l^2 = x_l \circ x_l$ is the vector of squared elements of x with \circ the Hadamard product. Right-multiplying both sides of Eq. (2) by this expression, and assuming that $\mathbb{E}[x_l x_l^\top]$ is indeed diagonal, we obtain

$$\Delta_{W_l} \text{diag}(\mathbb{E}[x_l^2]) = \mathbb{E}[z_l x_l^\top] - W_l \text{diag}(\mathbb{E}[x_l^2]).$$

We may equivalently write $\Delta_{W_l} \text{diag}(\mathbb{E}[x_l^2])$ as $\Delta_{W_l} \circ \mathbb{E}[x_l^2]$. This amounts to a rescaling of the elements of Δ_{W_l} and can be safely ignored when using sufficiently small or adaptive learning rates. This finally leads to our constrained parameter inference (COPI) learning rule

$$\Delta_{W_l}^{\text{copi}} = \mathbb{E}[z_l x_l^\top] - W_l \text{diag}(\mathbb{E}[x_l^2]), \quad (3)$$

which is solely composed of a correlational learning term and a weight decay term. COPI receives its name from the fact that there are two constraints in play. First, the availability of a target state z_l for each layer and, second, the requirement that the inputs x_l are decorrelated.

2.4 Input decorrelation

We did not yet address how to ensure that the inputs to each layer are decorrelated. To this end, we introduce a new input decorrelation method which transforms the potentially correlation-rich outputs y_{l-1} of the previous layer into decorrelated inputs x_l to the current layer using the transformation

$$x_l = R_l y_{l-1},$$

where R_l is a decorrelating lateral weight matrix.

Let us consider attempting to reduce the correlation in the output data, x_l , by measurement of its correlation and a shift toward lower correlation. In particular, consider a desired change in a given sample of the form

$$x_l \leftarrow x_l - \eta (\mathbb{E}[x_l x_l^\top] - \text{diag}(\mathbb{E}[x_l^2])) x_l,$$

where the expectations could be taken over the empirical distribution. We can shift this decorrelating transformation from the output activities x_l to the decorrelating matrix R_l . To do so, consider $x_l = R_l y_{l-1}$, such that we may write

$$\begin{aligned} x_l &\leftarrow x_l - \eta (\mathbb{E}[x_l x_l^\top] - \text{diag}(\mathbb{E}[x_l^2])) x_l \\ &\leftarrow R_l y_{l-1} - \eta (\mathbb{E}[x_l x_l^\top] - \text{diag}(\mathbb{E}[x_l^2])) R_l y_{l-1} \\ &\leftarrow (R_l - \eta (\mathbb{E}[x_l x_l^\top] - \text{diag}(\mathbb{E}[x_l^2]))) R_l y_{l-1}. \end{aligned}$$

We converge to the optimal decorrelating matrix R_l^* using an update $R_l \leftarrow R_l + \eta \Delta_{R_l}^{\text{copi}}$ with

$$\Delta_{R_l}^{\text{copi}} = -(\mathbb{E}[x_l x_l^\top] - \text{diag}(\mathbb{E}[x_l^2])) R_l.$$

Assuming that R_l is initialised symmetrically, for example with the identity matrix, this matrix update maintains the symmetry of R_l and hence we may equivalently write this as

$$\begin{aligned} \Delta_{R_l}^{\text{copi}} &= -(\mathbb{E}[x_l x_l^\top] R_l - \text{diag}(\mathbb{E}[x_l^2]) R_l) \\ &= -(\mathbb{E}[q_l x_l^\top] - R_l \text{diag}(\mathbb{E}[x_l^2])) \end{aligned} \quad (4)$$

with $q_l = R_l x_l$. This has exactly the same form as our previous COPI rule for learning the forward weights though now acting on the ‘inhibiting’ (note the negative sign in the weight update) lateral weights and using target states q_l . Note that in reality these lateral weights are not strictly ‘inhibitory’ in the neuroscientific sense, but act to reduce correlation by providing either positive or negative feedback. Hence, we are invoking the same principle to learn both the forward and lateral weights! In effect, the lateral weights are constantly inferring correlational structure within the activities of a layer of units and by updating their values are reducing it.

2.5 Error signals

Equation (3) expresses learning of forward weights in terms of target states z_l . However, without access to targets for each layer of a deep neural network model, one may ask how this learning approach could be applied. To this end, we assume that the target states can be expressed as

$$z_l = a_l + \delta_l$$

with δ_l an error signal which perturbs the neuron’s state in a desired direction. According to stochastic gradient descent (SGD), the optimal perturbation is given by

$$\delta_l^{\text{sgd}} = -\frac{d\ell}{da_l}$$

as this guarantees that the neuronal states are driven in the direction of decreasing loss. The error signal at the output layer is given by

$$\delta_L \triangleq \delta_L^{\text{sgd}} = -\frac{\partial \ell}{\partial a_L} = -\text{diag}(f'(a_L)) \frac{\partial \ell}{\partial y_L}.$$

Starting from $\delta_L^{\text{bp}} = \delta_L$, the SGD perturbation can be computed via backpropagation (BP) by propagating the error signal from output to input according to

$$\delta_l^{\text{bp}} = \frac{\partial a_{l+1}}{\partial a_l} \delta_{l+1}^{\text{bp}}$$

with

$$\begin{aligned} \frac{\partial a_{l+1}}{\partial a_l} &= \frac{\partial y_l}{\partial a_l} \frac{\partial x_{l+1}}{\partial y_l} \frac{\partial a_{l+1}}{\partial x_{l+1}} \\ &= \frac{\partial f(a_l)}{\partial a_l} \frac{\partial R_{l+1} y_l}{\partial y_l} \frac{\partial W_{l+1} x_{l+1}}{\partial x_{l+1}} \\ &= \text{diag}(f'(a_l)) R_{l+1}^\top W_{l+1}^\top. \end{aligned}$$

While this provides a gold standard for the optimal perturbation, ideally, we would like to replace this by more biologically-plausible credit assignment methods that do not make use of gradient information. To this end, we can make use of a variety of alternative methods. Each of these methods uses the same error signal δ_L for the output layer but propagates the error signal in the input direction using different proposal mechanisms. Examples of such mechanisms are described in the following.

Feedback alignment

Feedback alignment (FA) supposes that the perturbation from the previous layer can be propagated through fixed random top-down weights B_{l+1} instead of the transposed weight matrix $(W_{l+1}R_{l+1})^\top$ [21]. Hence, the layer-wise perturbations are propagated by

$$\delta_l^{\text{fa}} = \text{diag}(f'(a_l))B_{l+1}\delta_{l+1}^{\text{fa}}.$$

Direct feedback alignment (DFA) instead makes use of a random projection of the output node errors to the rest of the network [22]. That is, $\delta_l^{\text{dfa}} = \text{diag}(f'(a_l))B_{l+1}\delta_L^{\text{dfa}}$.

Target propagation

Target propagation supposes that credit is assigned by a top-down pass from the target output toward the input [13]. Supposing top-down (approximate) inverse weight matrices $B_{l+1} \approx (W_{l+1}R_{l+1})^{-1}$ exist for every layer l , this can be integrated with COPI using a perturbation

$$\delta_l^{\text{tp}} = f(B_{l+1}\delta_{l+1}^{\text{tp}}) - a_l,$$

which indicates a perturbation away from the current activation, a_l , and toward the inverse model $f(B_{l+1}\delta_{l+1}^{\text{tp}})$ of the perturbation from the layer above. Target propagation is not directly related to backpropagation but a more direct theoretical relationship can be established via GAIT propagation [31].

2.6 Stochastic COPI

Stochastic COPI replaces the expectations over the empirical distributions in Eqs. (3) and (4) by single data points, as in stochastic gradient descent (SGD). COPI training on single data points proceeds by computing the stochastic weight updates

$$\Delta_{W_l}^{\text{copi}} = z_l x_l^\top - W_l \text{diag}(x_l^2) \quad (5)$$

$$\Delta_{R_l}^{\text{copi}} = -(q_l x_l^\top - R_l \text{diag}(x_l^2)) \quad (6)$$

with target states $z_l = a_l + \delta_l$ and $q_l = R_l x_l$ given some suitable error signal δ_l . Figure 1 provides an overview of the computational operations that are in play. See Appendix A for a pseudo-algorithm. In practice, we train on minibatches instead of individual data points.

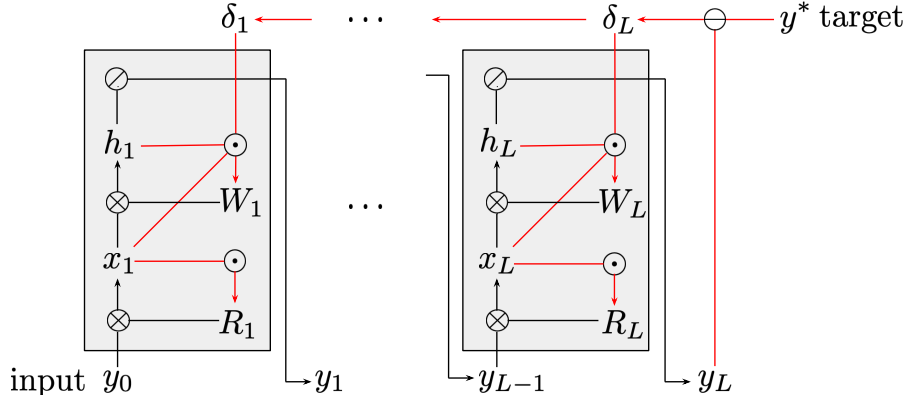


Figure 1: **COPI learning in a deep feedforward neural network.** Gray boxes represent COPI layers, with forward passes indicated in black and backward passes indicated in red. Parameter updates (5) and (6) indicated by \odot . Matrix multiplication indicated by \otimes . Activation function application indicated by \circ . Loss computation indicated by \ominus . Self-dependencies not shown.

2.7 Correspondence to stochastic gradient descent

It is instructive to consider (stochastic) COPI in the case of a single-layer neural network which is acting on decorrelated inputs. In this case, the forward pass is given by $y = f(a) = f(Wx)$ and the backward pass is given by $\Delta_W^{\text{copi}} = (a + \delta)x^\top - W \text{diag}(x^2)$. Recall that the SGD update of a single-layer network is given by

$$\Delta_W^{\text{sgd}} = -\frac{d\ell}{da}x^\top.$$

We can manipulate this expression to relate SGD to COPI as follows:

$$\begin{aligned} \Delta_W^{\text{sgd}} &= -\frac{d\ell}{da}x^\top \\ &= \left(a - \frac{d\ell}{da}\right)x^\top - ax^\top \\ &= (a + \delta^{\text{sgd}})x^\top - W(xx^\top). \end{aligned}$$

Clearly, in this special case, the SGD update and the COPI update with error signal δ^{sgd} are approximately equivalent, though SGD’s weight decay is modified by sample-wise input correlations and COPI explicitly assumes these to be a diagonal matrix.

3 Results

In the following, we analyse both the convergence properties of COPI and the benefits of the decorrelated representations at every network layer.

3.1 COPI performance on standard benchmarks

To validate (stochastic) COPI as a principle for learning, we compared it against backpropagation using fully-connected deep feedforward neural networks trained on the MNIST handwritten digit dataset [36] and the CIFAR-10 image dataset [10]. To isolate the impact of the learning signal, COPI was used together with both BP-based (δ_l^{bp}) and FA-based (δ_l^{fa}) perturbations with a loss function composed of the quadratic loss between network outputs and the one-hot encoded labels as ‘desired’ output.

To clarify the benefits of the COPI algorithms, we additionally apply our iterative decorrelation procedure to backpropagation itself. A baseline with backpropagation alone is also provided, where a network with no layer-wise decorrelating transformations is optimized with the Adam optimizer [14] for the same number of epochs as the other simulations. All plotted (non-Adam) curves use a vanilla non-adaptive implementation and are hence more comparable. The activation function used in this network was a leaky rectified linear unit (leaky-ReLU). The network transformation is further described in the methods above. Training was carried out in minibatches of size 50 for all simulations (stochastic updates computed within these minibatches and averaged during application). For the simulations involving the MNIST handwritten digit dataset, the learning rate of the simulations began at 10^{-2} for the first epoch to ensure that the decorrelation could set in, and was thereafter boosted to 10^{-1} for all simulations aside from Adam (constant learning rate: 10^{-4}). For CIFAR-10, learning rates underwent the same change but began at 10^{-3} and were increased to 10^{-2} after the first epoch. This learning rate adjustment after the first epoch was useful as unit activities are significantly reduced by the decorrelating procedure and this causes a lower effective learning rate. Thus, after an initial epoch of training which stabilised the decorrelation, we boosted the learning rates for all simulations which make use of decorrelation. Learning rates for the forward and lateral weight matrices were kept the same at all times.

Figure 2 shows the results of our experiments. The first thing to notice is that, during training, COPI is more successful as a learning rule compared to BP in the presence of decorrelation. We attribute this benefit to the explicit knowledge, built into the COPI learning rule, that inputs

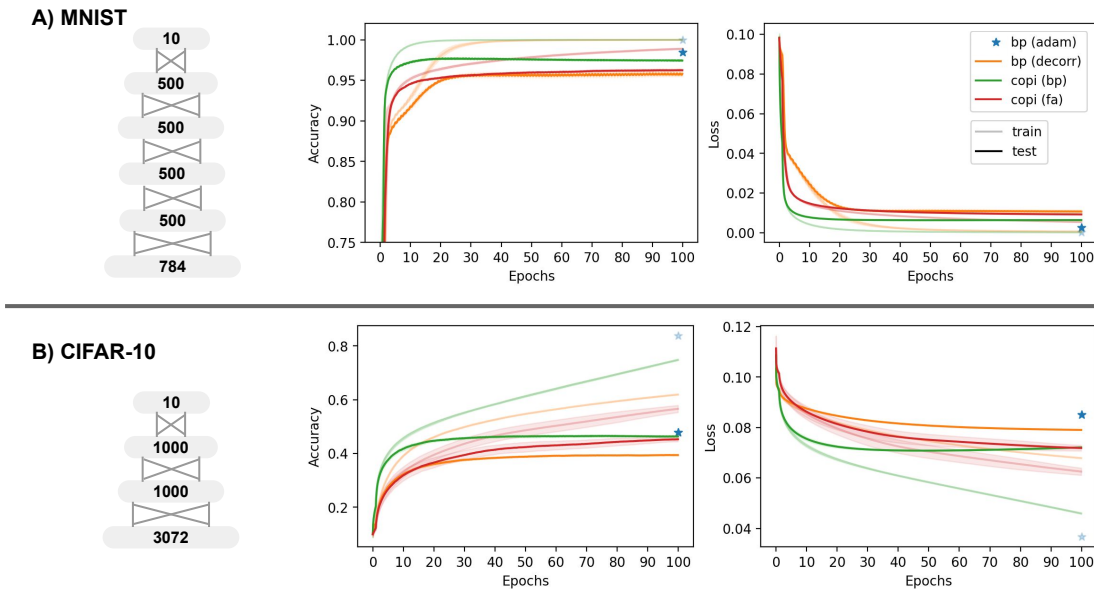


Figure 2: **COPI vs BP performance on standard computer vision classification tasks.** A) Train/test accuracy and loss of a five-layer (784-500-500-500-10, layer sizes), fully-connected, feedforward deep neural network model trained and tested on the handwritten MNIST dataset. B) Train/test accuracy of a three-layer (3072-1000-1000-10), fully-connected, feedforward deep neural network model trained and tested on the CIFAR-10 dataset. All networks were run with five random seeds and envelopes show standard deviation across these networks.

shall reach a decorrelated state. By comparison, BP updates are computed without this explicit knowledge and are therefore negatively affected by sample/mini-batch correlations.

Not only in terms of accuracy, but also in terms of speed, COPI shows rapid convergence. It is important to note that BP with momentum does converge faster in general, though we do not compare the speed of convergence to the momentum case as an investigation into momentum’s application to the decorrelating rule must yet be undertaken. Furthermore, test performance of COPI is on par with BP, though multiple methods begin to show signs of overfitting in this network setup. Third, competitive performance is even obtainable using feedback alignment, with a continuing benefit of the use of the COPI algorithm. This suggests that attempts to make the backpropagation signal more biologically plausible and local might prove successful with COPI.

3.2 Decorrelation for feature analysis and network compression

The COPI algorithm’s requirement for decorrelation at every network layer is not only a restriction but also proves beneficial in a number of ways. We explore the decorrelation, as well as the analyses and computations that it enables.

The proposed decorrelation method produces a representation similar to existing whitening methods, such as ZCA [6]. Figure 3A provides a visualisation of a randomly selected set of data samples from the MNIST dataset. Top to bottom are shown the unprocessed samples, samples processed by the first decorrelating layer of a network trained on MNIST with the COPI algorithm (see MNIST networks described in Figure 2), and finally a visualisation of samples transformed by a ZCA transform computed on the whole training set. As can be seen, there is qualitative similarity between the COPI- and ZCA-processed data samples. Remaining differences are attributed to the fact that COPI does not scale the individual elements of these samples (pixels) for unit variance.

Beyond the input transformation, our COPI setup allows some interesting analyses, courtesy

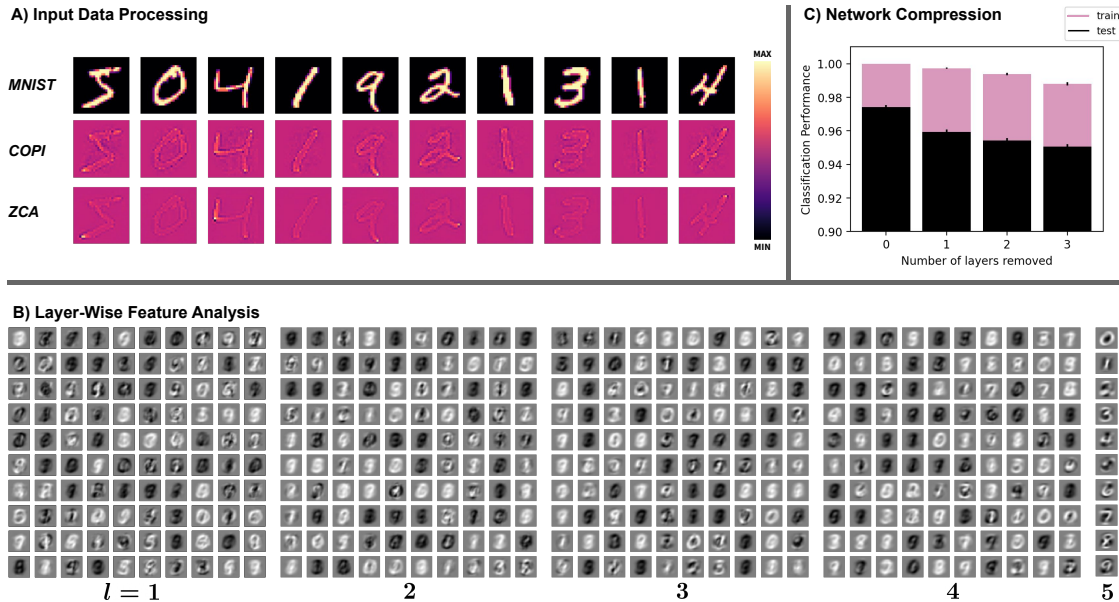


Figure 3: **The effect of whitening of the input layer activities, and decoded features across layers of a COPI network.** A) Visualisation of the MNIST dataset (top), the decorrelating transformation produced by the COPI algorithm (middle), and, for comparison, the whitening transformation produced by ZCA whitening (bottom). B) Given the decorrelated inputs, x_l , to every layer of a COPI trained network, the training set data was correlated with the layer-wise decorrelated inputs. This produced a ‘training-set derived basis set’ as the input to every network layer. These could then be combined using the layer weight matrix, W_l , to visualise the features detected by layers of a COPI network. C) The decorrelated layer-wise inputs of COPI-trained networks can be used to infer linear mappings between distant layers of the network. This allows the removal of layers of a network and replacement with an inferred, linearly approximation of those intermediate layers. Plotted are the performances of the 5-layer MNIST-trained COPI networks of Figure 2 with up to 3 hidden layers replaced with a single weight matrix. This process is repeated for all five, randomly seeded networks and standard deviation is shown with error bars.

of the decorrelated layer-wise inputs. For visualisation of receptive fields of units deep within the network, we can make use of layer-wise decorrelated responses x_l , in order to form a linear approximation of their average receptive field. For each decorrelated unit, that is, each element of x_l for a given layer l , we can correlate its activity with the input pixels across the entire training set. This provides an average, linear, feature response for each element of x_l in a given layer. These features can then be combined, using the weight matrices W_l , to determine feature preferences of the activations of units in the network, where the activations are computed as $a_l = W_l x_l$. Figure 3B shows such extracted features from a random selection of 100 units from each layer of a COPI-trained network (ten for the final layer, which only holds 10 units). This allows us to observe an increasingly digit-oriented feature preference for units in our COPI-trained network, as we go deeper into the network, and the presence of digit selective and ‘anti-digit’ selective units.

Furthermore, the decorrelation also provides a computationally simple method to approximate multiple layers of a COPI-trained network with a linear matrix. Appendix B explores how this approximation can be made. This allows us to easily convert a network of five layers into networks of any smaller number of layers, effectively providing a straightforward approach for network compression. Figure 3C shows the performance impact of such conversions when five-layer MNIST-trained COPI networks have their hidden layers successively removed and instead approximated with linear matrices. As can be seen, and without any additional retraining, the network performance stays high despite the approximation and removal of layers. The ability to

achieve this network compression efficiently is a unique benefit of the decorrelation of units at every network layer.

4 Discussion

In this paper, we introduced constrained parameter inference (COPI) as new approach to learning in feed-forward neural networks. Our approach was developed with a few key principles in mind. First, locality of information for weight updates. That is, we wish for all variables relevant to the update rule to be local to the parameter being learned. Second, the error signals must be integrated into the activity of units. This ensures the existence of some desirable output instead of requiring a separate error propagation mechanism that directly affects parameters.

We derived an effective local learning rule and showed that, under the right conditions, individual weights can infer their own values. The approach requires the removal of confounding influences between unit activities within every layer of the neural network. To this end, we derived an efficient iterative decorrelation rule which, itself, is a special case of constrained parameter inference. We further assume that an error signal is available which can perturb a unit’s activation towards a more desirable state. Here, a wide range of different proposal signals can be used.

The resulting algorithm allowed us to effectively train deep feedforward neural networks, where performance is competitive with that of backpropagation for both gradient-based and feedback alignment signals. The algorithm also allows for more interpretable deep learning via the visualisation of deep decorrelated features [30]. Furthermore, it contributes to efficient deep learning as it facilitates network compression [35].

COPI relates to unsupervised methods for subspace learning [2, 5, 16]. In particular, learning uncorrelated latent factors which capture our higher-resolution input can be viewed as a form of dimensionality reduction. Specifically, we are learning uncorrelated latent factors which capture our input. In particular, the form of the learning rule we propose bears a resemblance to Oja’s rule [2], see Appendix C for details, though it focuses on inference instead of latent factor extraction.

It is also interesting to note that our decorrelating mechanism captures some of the key elements of batch normalization [15, 25]. First, vanilla batch-normalization makes use of demeaning and variance-scaling. Furthermore, whitening of batches has been recently shown to be an extremely effective batch-wise processing stage, yielding state-of-the-art performance on a number of challenging classification tasks [25]. Thus, a whitening procedure as a whole has been suggested as a sensible preprocessing stage but has not yet been linked to weight inference as we do here.

Aside from unsupervised methods, the inference of parameters based upon input and output activities has been previously proposed to overcome the weight-transport problem [26, 28, 34]. In particular, these methods attempt to learn the feedback connectivity required for backpropagation via random stimulation of units and a process of weight inference. Our method similarly attempts to carry out weight inference, but does so for the learning of the forward model and combines this with top-down perturbation and inputs which are transformed to be decorrelated rather than random.

COPI may also shed light on learning and information processing in biological systems. There is both experimental and theoretical evidence that input decorrelation is a feature of neural processing through a number of mechanisms including inhibition, tuning curves, attention, and eye movements [6, 8, 9, 11, 12, 17, 18, 23, 27]. In particular, center-surround filters of the LGN appear to produce a form of whitening. This whitening also appears to be key for sparse coding of visual inputs. To what extent there is decorrelation between all units projecting to a neuron is of course questionable, though COPI has the potential for modification to account for global or local correlations.

Beyond this, evidence for preprocessing of inputs to early visual areas, inhibitory and excitatory balance [20] has been formulated in a fashion which can be viewed as encouraging whitening. Learning rules which capture excitatory/inhibitory balance, such as the one by Vogels et al. [11], rely on inhibition between units, which is tuned to reduce the inter-unit covariance. Thus, this inhibition is acting to set off-diagonal elements of the covariance matrix to zero. Such detailed

balance has been observed across cortical areas and so it does not seem unreasonable to consider this as a method to encourage decorrelation of not just the input but also downstream ‘hidden’ layers of neural circuits.

Concluding, we argue that constrained parameter inference is not only a prime candidate for biologically plausible learning using information that is locally available at the synapse but can also be treated as a plugin replacement of backpropagation for efficient and effective training of deep feedforward neural networks.

References

- [1] S. Linnainmaa. “The representation of the cumulative rounding error of an algorithm as a Taylor expansion of the local rounding errors”. In: *Master’s Thesis (in Finnish), Univ. Helsinki* (1970), pp. 6–7.
- [2] E. Oja. “Simplified neuron model as a principal component analyzer”. In: *Journal of Mathematical Biology* 15.3 (1982), pp. 267–273.
- [3] S. Grossberg. “Competitive learning: From interactive activation to adaptive resonance”. English. In: *Cognitive Science* 11.1 (1987), pp. 23–63.
- [4] F. Crick. “The recent excitement about neural networks”. In: *Nature* 337 (1989), pp. 129–132.
- [5] P. Földiák and M. P. Young. “Sparse coding in the primate cortex”. In: *The Handbook of Brain Theory and Neural Networks*. 1995.
- [6] A. J. Bell and T. J. Sejnowski. “The “independent components” of natural scenes are edge filters”. In: *Vision Research* 37.23 (1997), pp. 3327–3338.
- [7] P. J. Werbos. “Applications of advances in nonlinear sensitivity analysis”. In: *System Modeling and Optimization* (2005), pp. 762–770.
- [8] D. J. Graham, D. M. Chandler, and D. J. Field. “Can the theory of “whitening” explain the center-surround properties of retinal ganglion cell receptive fields?” In: *Vision Research* 46.18 (2006), pp. 2901–2913.
- [9] M. R. Cohen and J. H. R. Maunsell. “Attention improves performance primarily by reducing interneuronal correlations”. en. In: *Nat. Neurosci.* 12.12 (Dec. 2009), pp. 1594–1600.
- [10] A. Krizhevsky. *Learning multiple layers of features from tiny images*. Tech. rep. University of Toronto, 2009.
- [11] T. P. Vogels et al. “Inhibitory plasticity balances excitation and inhibition in sensory pathways and memory networks”. In: *Science* 334.6062 (2011), pp. 1569–1573.
- [12] X. Pitkow and M. Meister. “Decorrelation and efficient coding by retinal ganglion cells”. In: *Nature Neuroscience* 15.4 (2012), pp. 628–635.
- [13] Y. Bengio. “How auto-encoders could provide credit assignment in deep networks via target propagation”. In: *ArXiv* (2014). ArXiv: 1407.7906 (cs.LG).
- [14] D. P. Kingma and J. Ba. “Adam: A method for stochastic optimization”. In: *ArXiv* (2014). ArXiv: 1412.6980 (cs.LG).
- [15] S. Ioffe and C. Szegedy. “Batch normalization: Accelerating deep network training by reducing internal covariate shift”. In: *ArXiv* (2015), pp. 1–11. ArXiv: 1502.03167 (cs.LG).
- [16] C. Pehlevan, T. Hu, and D. B. Chklovskii. “A Hebbian/anti-Hebbian neural network for linear subspace learning: A derivation from multidimensional scaling of streaming data”. In: *ArXiv* (2015). ArXiv: 1503.00669 (q-bio.NC).
- [17] I. Y. Segal et al. “Decorrelation of retinal response to natural scenes by fixational eye movements”. en. In: *Proceedings of the National Academy of Sciences U.S.A.* 112.10 (2015), pp. 3110–3115.

- [18] R. Abbasi-Asl et al. “Do retinal ganglion cells project natural scenes to their principal subspace and whiten them?” In: *2016 50th Asilomar Conference on Signals, Systems and Computers*. 2016, pp. 1641–1645.
- [19] J. Brea and W. Gerstner. “Does computational neuroscience need new synaptic learning paradigms?” In: *Current Opinion in Behavioral Sciences* 11 (2016), pp. 61–66.
- [20] S. Denève and C. K. Machens. “Efficient codes and balanced networks”. In: *Nature Neuroscience* 19.3 (2016), pp. 375–382.
- [21] T. P. Lillicrap et al. “Random synaptic feedback weights support error backpropagation for deep learning”. In: *Nature Communications* 7 (2016), p. 13276.
- [22] A. Nøkland. “Direct feedback alignment provides learning in deep neural networks”. In: *Advances in Neural Information Processing Systems* 29 (2016).
- [23] K. Franke et al. “Inhibition decorrelates visual feature representations in the inner retina”. en. In: *Nature* 542.7642 (2017), pp. 439–444.
- [24] A. G. Baydin et al. “Automatic differentiation in machine learning: a survey”. In: *Journal of Machine Learning Research* 18 (2018), pp. 1–43.
- [25] L. Huang et al. “Decorrelated batch normalization”. In: *Proceedings of the IEEE Computer Society Conference on Computer Vision and Pattern Recognition* (2018), pp. 791–800.
- [26] M. Akrouf et al. “Deep learning without weight transport”. In: *ArXiv* (2019). ArXiv: 1904.05391 (cs.LG).
- [27] E. M. Dodds, J. A. Livezey, and M. R. DeWeese. “Spatial whitening in the retina may be necessary for V1 to learn a sparse representation of natural scenes”. In: *BioRxiv* (2019), pp. 1–15. DOI: [doi:https://doi.org/10.1101/776799](https://doi.org/10.1101/776799).
- [28] J. Guerguiev, K. P. Kording, and B. A. Richards. “Spike-based causal inference for weight alignment”. In: *ArXiv* (2019). ArXiv: 1910.01689 (q-bio.NC).
- [29] B. A. Richards et al. “A deep learning framework for neuroscience”. In: *Nature Neuroscience* 22.11 (2019), pp. 1761–1770.
- [30] C. Rudin. “Stop explaining black box machine learning models for high stakes decisions and use interpretable models instead”. In: *Nature Machine Intelligence* 1.5 (2019), pp. 206–215. arXiv: 1811.10154.
- [31] N. Ahmad, M. A. J. van Gerven, and L. Ambrogioni. “GAIT-prop: A biologically plausible learning rule derived from backpropagation of error”. In: *Advances in Neural Information Processing Systems* 33 (2020).
- [32] T. P. Lillicrap et al. “Backpropagation and the brain”. In: *Nature Reviews Neuroscience* 21.6 (2020), pp. 335–346.
- [33] V. Ranganathan and A. Lewandowski. “ZORB: A derivative-free backpropagation algorithm for neural networks”. In: *ArXiv* (2020). arXiv: 2011.08895 [cs.LG].
- [34] N. Ahmad, L. Ambrogioni, and M. A. J. van Gerven. “Overcoming the weight transport problem via spike-timing-dependent weight inference”. In: *NBDT* 5.3 (2021), pp. 1–20.
- [35] S. Wang. “Efficient deep learning”. In: *Nature Computational Science* 1.3 (2021), pp. 181–182.
- [36] Y. LeCun, C. Cortes, and C. J. Burges. *The MNIST database of handwritten digits*. AT&T Labs [Online]. Available: <http://yann.lecun.com/exdb/mnist>.

A COPI pseudocode

Algorithm 1 demonstrates COPI training of a deep feedforward neural network using a quadratic loss. For illustration, we use backpropagation-based perturbations δ_l^{bp} .

Algorithm 1 Constrained Parameter Inference

```

1: procedure COPI(network, data)
  ▷ network consists of randomly initialized forward weight matrices  $W_l$  and lateral weight matrices  $R_l$  with  $1 \leq l \leq L$ 
  ▷ data consists of  $N$  input-output pairs  $(y_0, y^*)$ 
  ▷ Parameters: learning rates  $\eta_R$  and  $\eta_W$ ; number of epochs; batch size
2:   for each epoch do
3:     for each batch =  $\{(y_0, y^*)\} \subset \textit{data}$  do
      ▷ Forward pass
4:       for layer  $l$  from 1 to  $L$  do
5:          $x_l = R_l y_{l-1}$                                      ▷ Decorrelate the input data
6:          $a_l = W_l x_l$                                        ▷ Compute activation
7:          $y_l = f(a_l)$                                        ▷ Compute output
8:       end for
9:        $\ell = \|y_L - y^*\|^2$                                      ▷ Compute loss
      ▷ Backward pass
10:      for layer  $l$  from  $L$  to 1 do
11:         $\delta_l = -\frac{d\ell}{da_L}$  if  $l = L$  else  $\delta_l = \frac{da_{l+1}}{da_l} \delta_{l+1}$    ▷ Compute learning signal
12:         $W_l \leftarrow W_l + \eta_W ((a_l + \delta_l)x_l^\top - W_l \text{diag}(x_l^2))$    ▷ Update forward weights
13:         $R_l \leftarrow R_l - \eta_R ((R_l x_l) x_l^\top - R_l \text{diag}(x_l^2))$    ▷ Update lateral weights
14:      end for
15:    end for
16:  end for
17: return network
18: end procedure

```

B Compressing COPI networks

Here we describe how the presence of decorrelated inputs at every network layer enables the compression of a network. Specifically, we make use of these decorrelated inputs in order to approximate multiple (non-linear) layer transformations with a linear matrix.

Consider a system in which one has access to some empirical dataset, $X \in \mathbb{R}^{M \times N}$, where M is the number of features and N the number of datapoints. Suppose also, that there exists some (potentially non-linear) transformation of this dataset, such that $Z = f(X) \in \mathbb{R}^{P \times N}$, where $f(\cdot)$ is some arbitrary function and P is the dimensionality of the transformed data. We could then suppose that we can compute a linear approximation of the function $f(\cdot)$, such that

$$Z \approx WX.$$

Supposing that we take this approximation for granted, we might then attempt to solve for the matrix W by

$$Z = WX \Rightarrow W = ZX^{-1}.$$

This would only be possible if X was invertible and square. Naturally, a pseudo-inverse could also be deployed, though this is expensive to compute. For such an approach to learning in deep networks, see [33].

Alternatively, we could (as carried out within the derivation of COPI) multiply our original formulation by the transpose of our data, such that

$$Z = WX \Rightarrow ZX^\top = WXX^\top \Rightarrow W = ZX^\top (XX^\top)^{-1},$$

where we have now shifted away from an inverse of the data to, instead, the inverse of its correlation matrix. However, we nonetheless still require an (expensive) computation of a matrix inverse. In the case of networks trained to have decorrelated inputs at every layer, we can choose these inputs as our input data, such that $(XX^\top)^{-1} = \text{diag}(1/x_1x_1^\top, \dots, 1/x_Mx_M^\top) \triangleq D$ for these layer activities with x_m the m th row of X . This allows us to compute a transformation from such decorrelated inputs as

$$W = ZX^\top D.$$

Thus, in networks with decorrelated layer-wise inputs or activities, linear approximations of transformations can be computed without computing inverses. This is ultimately the mechanism by which COPI also operates, though in a sample/batch-wise manner with a changing output distribution (due to the learning signals). Specifically, consider the COPI algorithm at its ‘fixed point’, where $\Delta_{W_l}^{\text{copi}} = 0 = \mathbb{E}[z_l x_l^\top] - W_l \text{diag}(\mathbb{E}[x_l^2])$. Under this condition, we could re-arrange to say that $W_l = \mathbb{E}[z_l x_l^\top] \text{diag}(\mathbb{E}[x_l^2])^{-1}$, equivalent to our above formulation but under the assumption that we have a fixed, desired output, z_l , unlike the case where we wish to compute stochastic errors and do online learning.

The MNIST dataset consists of many input pixels with a consistently zero activation across all data samples (in the periphery). Due to this, the removal of hidden layers was carried out by removal of layers following the first network layer and the first network layer was never removed. This ensured that our decorrelated data, X , used for the determination of a linear approximation, had no elements which were zero and thus we could divide by X without issue.

C Single-weight updates

Let us consider the COPI update for single synaptic weights, given by

$$\begin{aligned} \Delta_{w_{ij}}^{\text{copi}} &= z_i x_j - w_{ij} x_j^2 = \left(\sum_j w_{ij} x_j \right) x_j - w_{ij} x_j^2 + \delta_i x_j \\ \Delta_{r_{ij}}^{\text{copi}} &= -(\tilde{z}_i x_j - r_{ij} x_j^2) = \left(\sum_j (-r_{ij}) x_j \right) x_j - (-r_{ij}) x_j^2. \end{aligned}$$

The first term in both expressions is a Hebbian update which relies on the states of the pre-synaptic units x_j and post-synaptic units z_i or \tilde{z}_i only. The second term in both expressions takes the form of a weight decay. This functional form is similar to Oja’s rule [2], which states:

$$\Delta_{m_{ij}}^{\text{oja}} = y_i x_j - m_{ij} y_i^2 = \left(\sum_j m_{ij} x_j \right) x_j - m_{ij} y_j^2$$

for $y = Mx$. COPI differs from Oja’s rule in that the forward weight update has an additional term $\delta_i x_j$ and the weight decay for both the forward and lateral weights depends on the (squared) pre-synaptic rather than post-synaptic firing rates. The functional impact of the difference in the weight decay scaling (by post- vs pre-synaptic firing rates), is that Oja’s rule scales weight decay in order to normalize the scale of the weights which target a post-synaptic neuron. By comparison, COPI scales the weight decay in order to best infer the scale which the weights should take in order to reproduce the post-synaptic neuron activity given the observed pre-synaptic neuron activity.